OLD DOMINION UNIVERSITY RESEARCH FOUNDATION

DEPARTMENT OF PHYSICS AND GEOPHYSICAL SCIENCES
SCHOOL OF SCIENCES AND HEALTH PROFESSIONS
OLD DOMINION UNIVERSITY
NORFOLK, VIRGINIA

Technical Report PGS-TR-PH-75-16

A HIGH-TEMPERATURE WIDEBAND PRESSURE TRANSDUCER

By

Allan J. Zuckerwar

Prepared for the
National Aeronautics and Space Administration
Langley Research Center
Hampton, Virginia

Under
Grant NSG 1039
March - September 1975

November 1975

DEPARTMENT OF PHYSICS AND GEOPHYSICAL SCIENCES
SCHOOL OF SCIENCES AND HEALTH PROFESSIONS
OLD DOMINION UNIVERSITY
NORFOLK, VIRGINIA

Technical Report PGS-TR-PH-75-16

A HIGH-TEMPERATURE WIDEBAND PRESSURE TRANSDUCER

By

Allan J. Zuckerwar

Prepared for the
National Aeronautics and Space Administration
Langley Research Center
Hampton, Virginia 23665

Under
Grant NSG 1039
March - September 1975
H.K. Holmes, Technical Monitor
Instrument Research Division

Submitted by the
Old Dominion University Research Foundation
Norfolk, Virginia 23508

November 1975

A HIGH-TEMPERATURE WIDEBAND PRESSURE TRANSDUCER

1. INTRODUCTION

The objective of NSG 1039 is to develop a pressure transducer for measurement of the pressure fluctuations in the high-temperature environment of a jet exhaust. A previously developed condenser microphone carrier system will be adapted to meet the specifications defined in a preceding progress report: A.J. Zuckerwar, Progress Report 9/74 - 3/75, NASA Grant NSG 1039, "A High-Temperature Wideband Pressure Transducer."

In addition, the following public disclosures of research performed under this grant have been or will be presented: N.V. Cohen, "Analytical and Experimental Study of Capacitance Microphones," 53rd Annual Meeting of the Virginia Academy of Sciences, p. 13 of program; and A.J. Zuckerwar, "Self-Consistent Approach to the Problem of Membrane-Fluid Coupling in Condenser Microphones," to be presented at the Ninetieth Meeting of the Acoustical Society of America, November 4-7, 1975.

The research tasks for the third and fourth quarters of the grant may be summarized as follows:

a. To operate the carrier system using the cable between the microphone cartridge and converter as a half-wavelength transmission line.

b. To determine the essential acoustical specifications of a prototype microphone cartridge at room temperature.

c. To complete the analytical study of the condenser microphone cartridge as a basis for optimal design.

d. To construct a facility for testing the microphone cartridge at elevated temperatures.

Construction and preliminary testing of a prototype microphone cartridge (task b) and the analytical study (task c) have been completed; operation of the cable as a half-wavelength transmission line (task a) has been demonstrated as feasible in principle, but the quality of the output signal is not yet sufficient to meet specifications. High-temperature testing (task d) must be

deferred until the cable problem is resolved. Details are discussed in the remaining sections of this report.

2. THEORETICAL BACKGROUND

An extensive search of the literature has revealed that a theoretical analysis describing the operation of the condenser microphone in terms of geometry, materials, and other physical properties is not yet available. The strong coupling between the motions of the membrane and underlying air layer, together with the difficult and unusual boundary conditions at the backplate, render the exact solution to the problem so complex as to be of little use to the designer. One of the objectives of the current research is to overcome these difficulties through realistic, physically sound simplifications, and to express the microphone sensitivity (membrane displacement over incident acoustical sound pressure) in terms of the parameters mentioned above.

Figure 1 shows a cross section of a conventional condenser microphone. Incident sound excites motion of the membrane, which compresses or expands the air in the gap and creates a "reaction pressure." The latter, resisting the motion of the membrane, is partially relieved by the flow of air through the openings in the backplate, and these determine the damping of the coupled membrane-air system. The prototype cartridge used in the current research has a single ring of four evenly spaced holes in the backplate.

Robey was the first to solve the fluid dynamical problem (ref. 1), but his unrealistic microphone model makes his results inapplicable to actual microphone design. In two papers, Petritskaya (refs. 2 and 3) gives an exact solution to the coupled problem, even for the case of an arbitrary arrangement of openings in the backplate[1], but his results are of such complexity that he does not give the membrane eigenfunctions and only presents numerical results for a particular microphone design. The analysis presented here differs from that of Petritskaya in two respects: first, the boundary condition at the backplate is more exact, and secondly, the reaction pressure term in the membrane equation is approximated

[1] Provided the openings have small radial dimensions, e.g., holes or annular slots.

in such a fashion as to allow a simple solution in closed form. Only a brief outline of the analysis will be presented here; full details will be deferred until the final report.

To derive the fluid dynamical equations we express the particle velocity in terms of a scalar potential ϕ and a vector potential $\vec{A}$,

$$\vec{v} = -\nabla\phi + \vec{A}$$

and insert these into the Navier-Stokes, continuity, and state equations to arrive at the following[1]:

$$\nabla^2\phi + k^2\phi = 0 \tag{1a}$$

$$\nabla^2\vec{A} + L^2\vec{A} = 0 \quad . \tag{1b}$$

Eq. (1b) is true if we impose the additional condition that $\vec{A}$ be solenoidal:

$$\nabla \cdot \vec{A} = 0 \quad .$$

Eqs. (1a) and (1b) lead to standard solutions to the Helmholz equation in cylindrical coordinates.

We write the boundary conditions in terms of the radial and axial components of particle velocity:

$$\begin{aligned} &v_r(r = a) = v_r\ (z = 0) = v_r\ (z = h) = 0 \\ &v_z(z = 0) = i\omega\eta(r,\theta), \qquad v_z(z = h) = f(r,\theta) \quad . \end{aligned} \tag{2}$$

The function $f(r,\theta)$, introduced by Petritskaya, describes the vertical component of the particle velocity at the backplate, and is shown at the bottom of figure 1. The velocity is assumed to have a constant value f_k ($k = 1, 2, \ldots q$) over the area of the kth opening and to equal zero at the solid portions of the backplate.

---

[1] A list of symbols appears at the end of this report.

Petritskaya assumes that the velocity f_k depends only upon the potential ϕ_k at the kth opening[1]:

$$f_k = \frac{i\rho_o \omega \phi_k}{Z_k s_k} \tag{3}$$

Because ϕ_k, in turn depends upon all the f_k's, the latter are coupled through a set of q simultaneous equations in q unknowns, where q is the number of openings in the backplate. Equation (3) neglects the fact that the volume velocities associated with the openings are coupled in the backchamber. Figure 2 shows an equivalent acoustic circuit of the backplate and backchamber. Solution to the circuit problem yields the result

$$f_k = \frac{i\rho_o \omega}{s_k} \sum_{\ell} Y_{k\ell}\, \phi_\ell \,. \tag{4}$$

Thus the f_k's are coupled below as well as above the backplate, for each ϕ_ℓ, as before, still depends upon all the f_k's. Equation (4) will lead to a more accurate prediction of the microphone response than equation (3).

The membrane equation contains two forcing terms, the driving force term due to the incident sound and the reaction pressure term:

$$\nabla^2 \eta + \kappa^2 \eta = -\frac{F_o}{T} + \frac{p}{T} \quad , \tag{5}$$

where the reaction pressure

$$p = i\rho_o \omega \phi(r, \theta, o)$$

depends upon the scalar potential. This term, however, is related to an integral containing η:

---

[1] The acoustical impedance Z_k is the ratio of the acoustic pressure $p_k = i\rho_o \omega \phi_k$ to the volume velocity $v_k = f_k s_k$.

$$\phi(r,\theta,o) = \sum_{m,n=0}^{\infty} \left[-i\omega\, \eta_{n,m} + \sum_{k=1}^{q} f_k\, R_{k,n,m} \right] \frac{J_{nb}\,(\xi_{n,m}\, r)\, \cos nb\theta}{T_{n,m}\, P_{n,m}} \quad , \qquad (6)$$

where

$$\eta_{n,m} = \int_0^{2\pi} \int_0^{a} \eta\,(r,\,\theta)\, J_{nb}\,(\xi_{n,m}\, r)\, \cos nb\theta\, r\, dr\, d\theta \quad . \qquad (7)$$

The boundary conditions for the membrane displacement are the following:

$$\eta\,(r = a) = 0 \quad , \quad \eta'\,(r = 0) \text{ is finite.} \qquad (8)$$

If we attempt to solve the membrane problem by expanding F_o and $\phi\,(r,\theta,o)$ in terms of the membrane eigenfunctions[1], then equations (5), (6), and (7) lead to an infinite set of simultaneous equations in an infinite number of unknowns. A self-consistent approach has been suggested (ref. 4) to overcome these difficulties. The proposed analysis is based upon two key simplifying assumptions:

a. η is assumed independent of θ. The effect of local variations in reaction pressure at the openings in the backplate is assumed to be smoothed out by the membrane tension. This assumption leads to the removal of the index n in equations (6) and (7).

b. The reaction pressure is assumed relatively insensitive to the details of the shape of the membrane. In equation (7), η will be represented by a simple expression, which contains a single unknown η_o and which retains the basic features of the membrane displacement (extremum at the center, zero at the periphery).

Actually, three different trial expressions for η have been investigated:

a. Constant: $\eta = \eta_o$. Here we assume that the reaction pressure depends only upon the average value of the displacement, but not its shape (ref. 5, p. 200).

b. Parabolic: $\eta = \eta_o \left(1 - \frac{r^2}{a^2}\right)$. This is the simplest polynomial fulfilling the requirements at the center and periphery.

---

[1] This may be the method used by Petritskaya, although details are not given.

c. Bessel: $\eta = \eta_0 \left[J_0 (Kr)/J_0 (Ka) - 1 \right]$. Here we assume that the effect of the reaction pressure is to change the amplitude, but not the shape, of the membrane displacement.

Substitution of a trial expression into Equation (7) permits a straightforward solution for η in Equation (5) in terms of the single unknown η_0, which can be eliminated if we require that the average value of η, as obtained from Equation (5), be the same as that obtained from the trial function. The latter can be expressed in terms of a "shape" factor B:

$$\langle \eta \rangle = B\eta_0 ,$$

where

$B = 1$ for case (a) (constant),

$= \frac{1}{2}$ for case (b) (parabolic),

$= J_2 (Ka)/J_0 (Ka)$ for case (c) (Bessel).

After elimination of η_0 the solution for $\langle \eta \rangle$ takes the following familiar form (ref. 5, page 202):

$$\langle \eta \rangle = \frac{\pi a^2 F_0}{-i\omega z_m} , \tag{9}$$

where z_m is the mechanical impedance of the membrane-air layer system.

$$z_m = \frac{\pi a^2 TK^2}{-i\omega} \left[\frac{J_0 (Ka)}{J_2 (Ka)} + D_1 + D_2 + D_3 + D_4 \right] \tag{10}$$

D_1 = air compliance term ,

D_2 = term accounting for motion of air through openings in backplate ,

D_3 = correction to D_1 accounting for curvature of membrane ,

D_4 = correction to D_2 accounting for curvature of membrane .

The frequency dependence of the average membrane displacement, computed from equations (9) and (10), is shown for each of the trial expressions in figure 3. We note that η = constant (case a) tends to underestimate the damping, and that the parabolic and Bessel expressions (cases b and c) show excellent agreement with one another right through the first membrane resonance.

At frequencies well below the first membrane resonance $\omega << 2.4048\ C_m/a$ the Bessel functions in equation (10) can be approximated by the first few leading terms in their power series expansions. The acoustical impedance becomes

$$z_m = \frac{z_m}{(\pi a^2)^2} = i\omega \frac{4}{3}\frac{\sigma}{\pi a^2} + \frac{8\pi T}{i\omega\,(\pi a^2)^2} + \frac{1}{i\omega}\frac{8\pi T}{(8\pi a^2)^2}(D_1 + D_2 + D_3 + D_4) \ . \qquad (11)$$

This representation suggests the lumped parameter equivalent circuit shown in figure 4 and valid below the first membrane resonance. The first two terms in equation (11) are associated with the membrane mass and compliance, the terms in D_1 and D_3 with the air layer, and D_2 and D_4 with the backplate and backchamber. The last of these are transformed in the figure from a series to a parallel representation in order to obtain nearly frequency-independent elements at low frequencies. As the frequency approaches 10 kHz , the backplate and backchamber reactance turns inductive, suggesting a possible Helmholz resonance near this frequency.

3. COMPARISON WITH EXPERIMENT

The preceding theory has been used as the basis for design of a prototype high-temperature microphone. An assembly drawing of the microphone cartridges tested is shown in the progress report referred to in the introduction.

Figure 5 shows a block diagram of the instrumentation used to measure the frequency response of the microphone by the electrostatic actuator technique. The microphone membrane is excited into vibration at a selected frequency by an ac signal originating at the oscillator, amplified by the power amplifier, superimposed upon an 800 V polarization voltage in the microphone calibration apparatus, and applied to the electrostatic actuator. Motion of the membrane is detected by the converter-zero drive system, described in detail in references 6 and 7. Because the connection between the microphone and converter is unavoidably

unshielded in this experiment, the spurious electrical pickup, which proves to be considerable, requires filtering. The highpass and lowpass sections of the filter are adjusted at each frequency to provide a third-octave bandwidth. After some amplification by the oscilloscope plug-in unit, the magnitude of the response is measured on a true rms voltmeter; with the output of the power amplifier serving as a reference, the phase is measured at the output of the filter. For the purpose of determining the attenuation and phase shift of the filter alone, measurements are taken with a reference signal applied directly from the oscillator to the input of the filter after each change in frequency. The automatic counter is used to measure the oscillator frequency. Identification of all the instruments in the system is included in the caption of figure 5.

The response of several prototype microphones, fabricated in the Instrument Development Section, Langley Research Center, has been compared to theoretical predictions. The values of the parameters entering equation (9) are listed in table 1. Two of the parameters readily permit adjustment: the gap distance by means of the threaded shaft supporting the backplate; and the membrane tension by means of the threaded ring, which applies pressure to the tension ring (see figure 1 of previous progress report). The gap distance is determined by measurement of the static capacitance between the membrane and backplate:

$$h = \frac{a^2}{36 \times 10^9 C} .$$

The membrane tension is determined by measurement of the first vacuum resonant frequency (for which the experimental arrangement of figure 5 was also used):

$$T = 6.825\ a^2 f_1^2 \rho_o t$$

Figure 6 shows the theoretical and experimental microphone frequency response for two different gap distances. Because of the difficulty in obtaining an absolute calibration of the membrane displacement, the experimental data for each microphone were multiplied by a constant calibration factor to fit the theory at a frequency of 10 Hz. The figure shows that the theory accurately predicts the height of the membrane resonance peak for both gap distances as well as the shift in peak location with increasing damping. The increase in damping with decreasing gap distance is expected in view of the role of viscosity in the flow between the membrane and backplate.

Figure 7 shows the response for two different membrane tensions at constant gap distance. Again both the height of the resonance peak and the shift in peak location show good agreement between theory and experiment. The change in membrane tension has two effects, both apparent in the figure: first the resonant frequency increases as the square root of the tension; secondly the sensitivity below resonance decreases with tension. The peak height does not change with tension because the latter has but negligible effect upon the damping.

Figure 8 shows the frequency dependence of the phase angle between applied driving force and membrane displacement. Theory accurately predicts the frequency at which the phase goes through the resonance step. The high experimental values on the high-frequency side of resonance are believed to contain a contribution from the zero drive amplifier, which produces some phase shift at frequencies approaching 20 kHz.

The theoretical and experimental results presented here lead to two conclusions:

a. The close agreement between the theoretical curves of those trial functions which satisfy the boundary requirements (cases 2 and 3) supports assumption b, i.e., that the reaction pressure is relatively insensitive to the details of the shape of the membrane.

b. Accurate prediction of the relative microphone response, and changes therein with changes in parameters, substantiates the self-consistent approach and the assumptions upon which it is based.

4. INVESTIGATION OF THE HIGH-TEMPERATURE CABLE

The hostile environment in which the microphone cartridge will eventually operate necessitates that the converter-zero drive system be removed from the microphone by a distance of at least 25 feet. A major effort of the current research is directed at studying the feasibility of connecting the microphone to the converter over a high-temperature cable operating as a half-wavelength transmission line.

The first type of cable investigated was a type "Q" high-temperature wire, manufactured by Maser Cable Co. This is a coaxial cable with a solid outer conductor, quartz fiber insulator, and stainless steel braided shield.

The temperature rating of the cable is 2000°F. Attempts to operate this cable as intended, however, have failed owing to the poor insulation between the center and outer conductors. The unloaded line resistance of a 25-foot section of cable measures less than 10kΩ; such a low value reduces the Q of the converter tank circuit to such an extent as to make the converter inoperable.

For the purpose of determining the feasibility of operating a microphone at the end of a half-wavelength transmission line, tests were conducted with a B & K type 4147 half-inch microphone connected to the converter over an approximately 25-foot length[1] of RG-58C/U cable. A comparison of the noise floor (which includes room noise) and 4% distortion level with and without the long cable are listed below:

	Without Cable	With Cable
Noise floor [dB]	86	110
SPL @ 4% distortion [dB]	154	164

From this table it is evident that the effect of the cable is to contribute noise to and reduce the sensitivity of the system.

A second type of high-temperature cable was manufactured in the Electronics Section of the Fabrication Division at Langley Research Center. A cross section of this cable is shown in figure 9. The center conductor A is bare copper wire. The insulators B are steatite ball and socket insulating beads (.125 inch diameter × .056 bore × .125 length). The outer conductor C is a braided shield made of inconel 600 with a 90% coverage factor. The microphone system, using this cable, was found to function, but the length of cable tested was far from a half wavelength. The proper cable length is currently being determined by time domain reflectometry.

5. FUTURE WORK

Work in the first two quarters of the grant extension will concentrate on the following areas of investigation:

a. To modify the microphone cartridge to achieve the goals of (1) extending the frequency response beyond 20 kHz, and (2) extending the dynamic range to the

[1] This length is a half wavelength at the carrier frequency of 9.008 MHz.

REFERENCES

1. D. H. Robey, J. Acoust. Soc. Am. 26, 740-745 (1954).

2. I. G. Petritskaya, Soviet Phys. - Acoust. 12, 193-198 (1966).

3. I. G. Petritskaya, Soviet Phys. - Acoust. 14, 105-106 (1968).

4. A. J. Zuckerwar, to be presented at the Ninetieth Meeting of the Acoust. Soc. Am., Nov. 4-7 (1975).

5. P. M. Morse, *Vibration and Sound* 2d Ed, McGraw-Hill (1948).

6. A. J. Zuckerwar and W. W. Shope, IEEE Trans. Instrum. Meas., IM-23, pp. 23-27 (1974).

7. A. J. Zuckerwar, "Automatic Tuning and Remote Calibration of a Microphone Carrier System," Final Technical Report NAS1-11707-29 (1974).

Table 1. Parameters of prototype microphone cartridge.

a	membrane radius	4.7625×10^{-3} m
t	membrane thickness	5.588×10^{-6} m
ρ_m	membrane density	7.9×10^{3} kg/m^3
σ	membrane surface density	4.4145×10^{2} kg/m^2
ρ_0	air density	1.21 kg/m^3
η	air viscosity coefficient	1.86×10^{-5} N sec/m^2
c	air sound velocity (isothermal)	2.8735×10^{2} m/sec
b	number of holes	4
r_1	hole location	2.6924×10^{-3} m
r_0	hole radius	3.969×10^{-4} m
ℓ_1	hole depth	6.604×10^{-4} m
r_2	slot location	4.667×10^{-3} m
t_2	slot width	9.525×10^{-5} m
ℓ_2	slot depth	6.604×10^{-4} m
v	volume of backchamber	1.4878×10^{-7} m^3

Adjustable: h air gap
T membrane tension

LIST OF SYMBOLS

a	radius of membrane [m]
$\vec{A}$	vector velocity potential
b	number of holes in ring in backplate
B	shape factor
C	static capacitance between membrane and backplate [Farad]
D_1, D_2, D_3, D_4	contributions to mechanical impedance from air layer and openings in backplate
f_1	first membrane resonant frequency in vacuum [Hz]
$f(r,\theta)$	distribution of vertical component of particle velocity at backplate surface [m/sec]
f_k	vertical component of particle velocity at kth opening in backplate [m/sec]
F_0	incident sound pressure [N/m^2]
h	gap distance between membrane and backplate [m]
$J_Q(X)$	Bessel function of first kind of order Q and argument X
k	wave number of sound in air [m^{-1}]
k	index used to designate openings in backplate
K	wave number of sound in membrane [m^{-1}]
L	$= (-i\omega/\nu)^{1/2}$ = wave number for vector potential [m^{-1}]
m	index used to designate roots of Bessel function $J_{nb}(\xi_{n,m}\, a) = 0$
n	index used to designate order of Bessel function
p	acoustical reaction pressure [N/m^2]
$P_{n,m}$	see reference 2, equation (4)
q	total number of openings in backplate

r	radial cylindrical coordinate [m]
$R_{k,n,m}$	see reference 2, equation (4)
s_k	area of kth opening in backplate
t	thickness of membrane [m]
T	tension of membrane [N/m]
$T_{n,m}$	see reference 2, equation (4)
$\vec{v}$	acoustical particle velocity [m/sec]
v_r	radial component of acoustical particle velocity [m/sec]
v_z	axial component of acoustical particle velocity [m/sec]
$Y_{k\ell}$	acoustical transfer admittance [m^5/N sec]
z	axial cylindrical coordinate [m]
z_m	mechanical impedance of the membrane - air layer system [N sec/m]
Z_k	acoustical impedance of kth opening in backplate [N sec/m^5]
Z_m	acoustical impedance of the membrane - air layer system [N sec/m^5]
$\eta = \eta(r,\theta)$	displacement of membrane [m]
$\eta_{n,m}$	coefficient in Fourier expansion of η
η_o	unknown in trial expression for membrane displacement [m]
θ	angular cylindrical coordinate
$\xi_{n,m}$	used to designate roots of Bessel function $J_{nb}(\xi_{n,m} a) = 0$ [m^{-1}]
ρ_o	static density of air [kg/m^3]
σ	surface density of membrane [kg/m^2]
$\phi = \phi(r,\theta,z)$	scalar velocity potential
ϕ_k	scalar velocity potential at kth opening in the backplate
ω	angular frequency of incident sound [sec^{-1}]

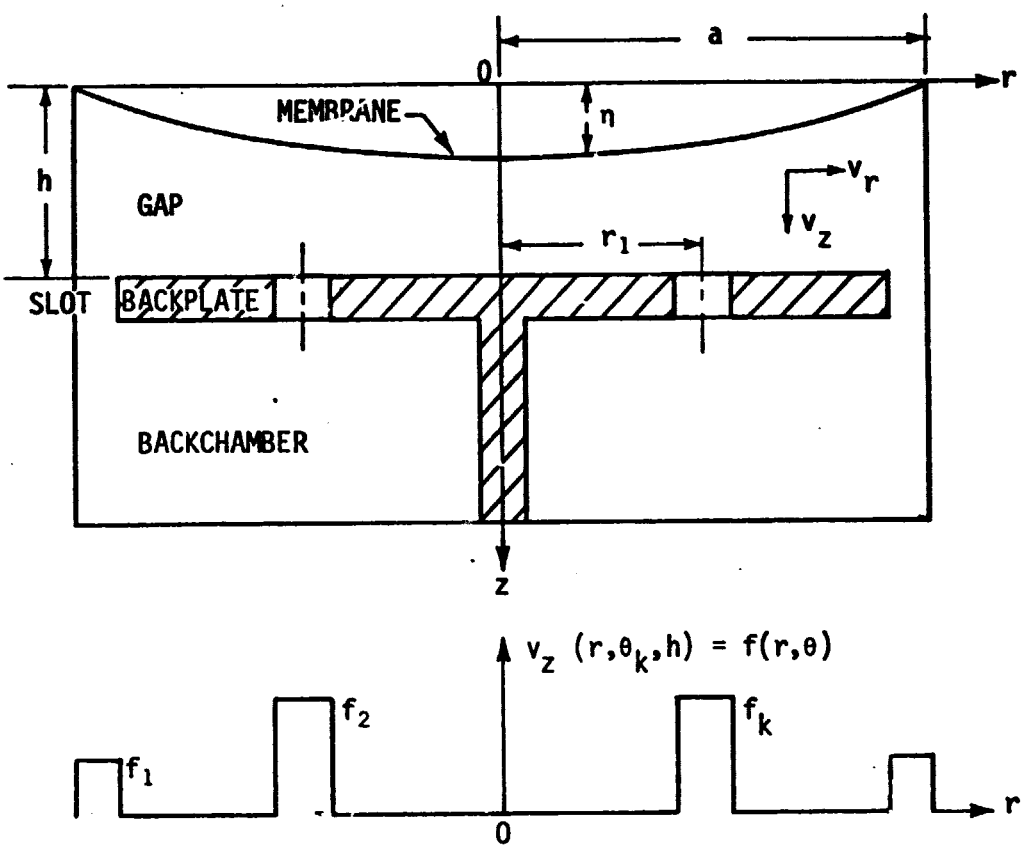

Figure 1. Cross section of prototype condenser microphone and profile of vertical velocity at backplate.

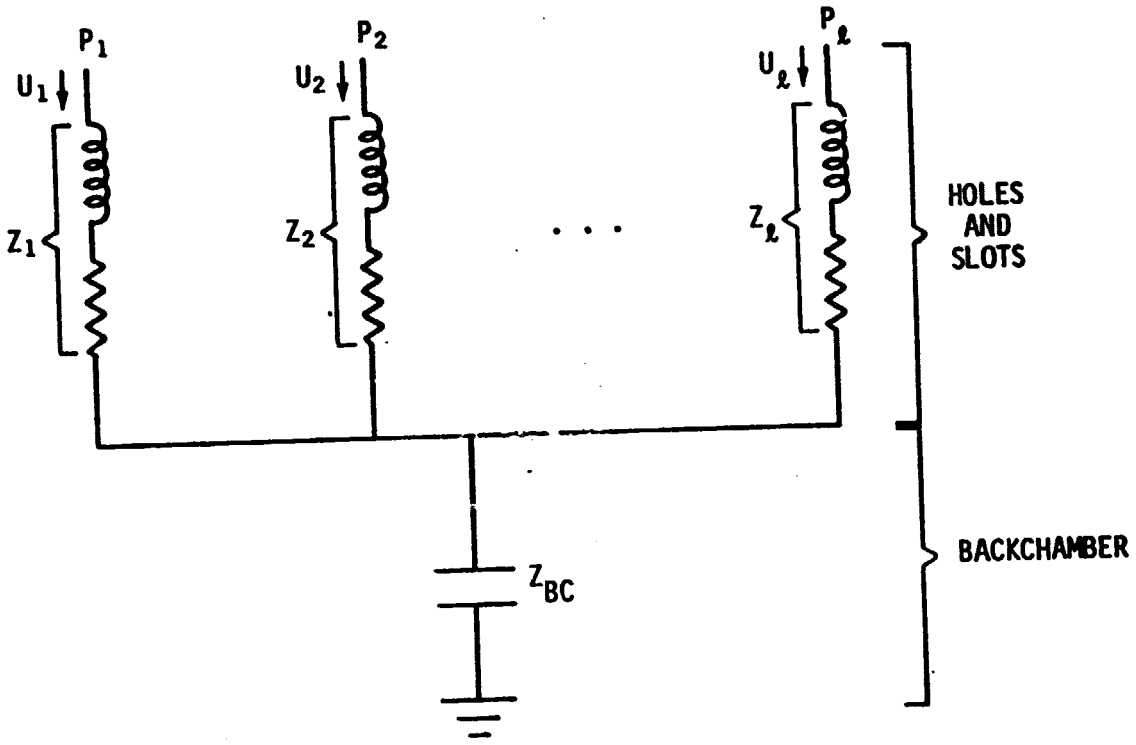

Figure 2. Equivalent circuit of backplate and backchamber.

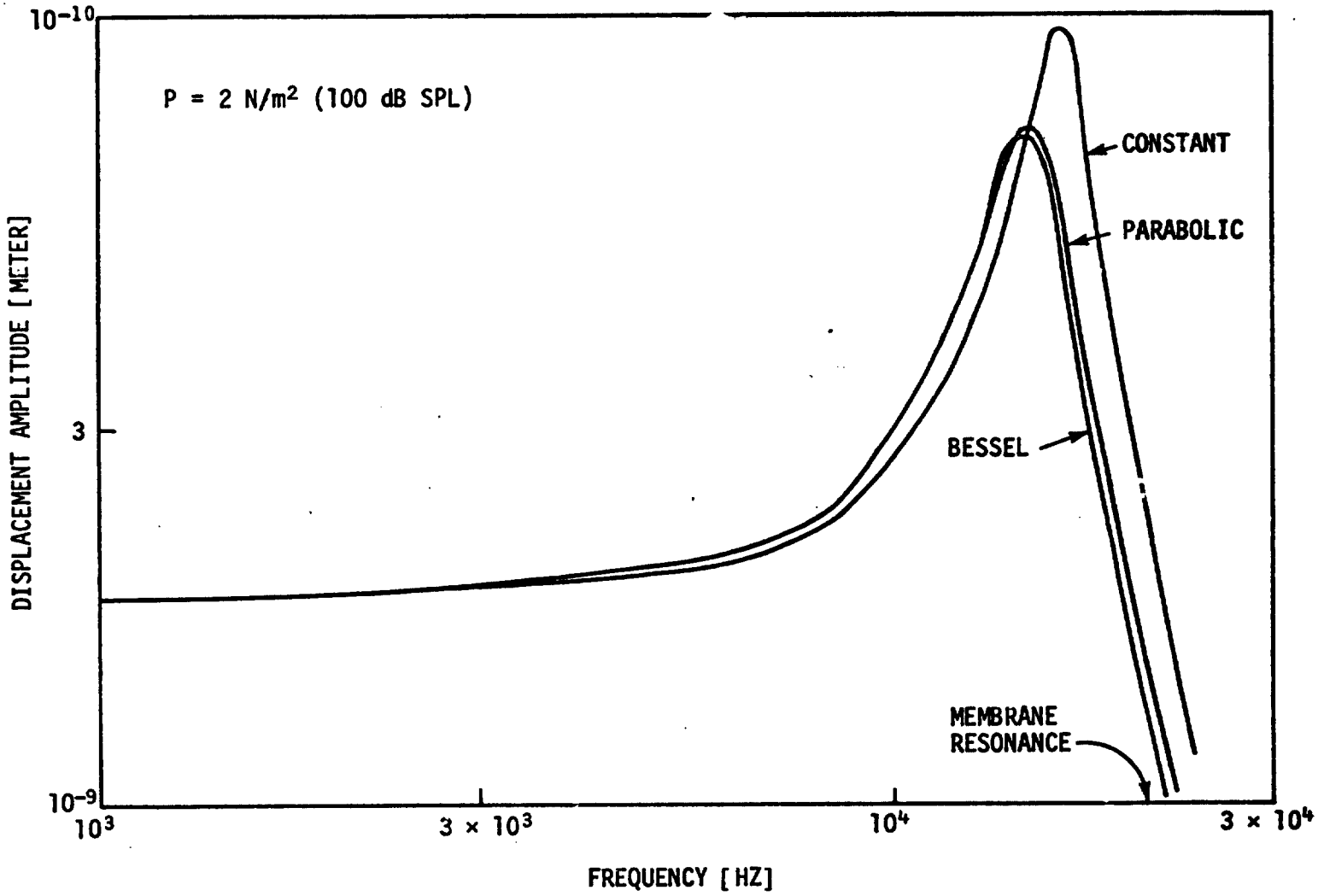

Figure 3. Frequency dependence of average membrane displacement for the constant (1), parabolic (2), and Bessel (3) trial expressions entering equation (7).

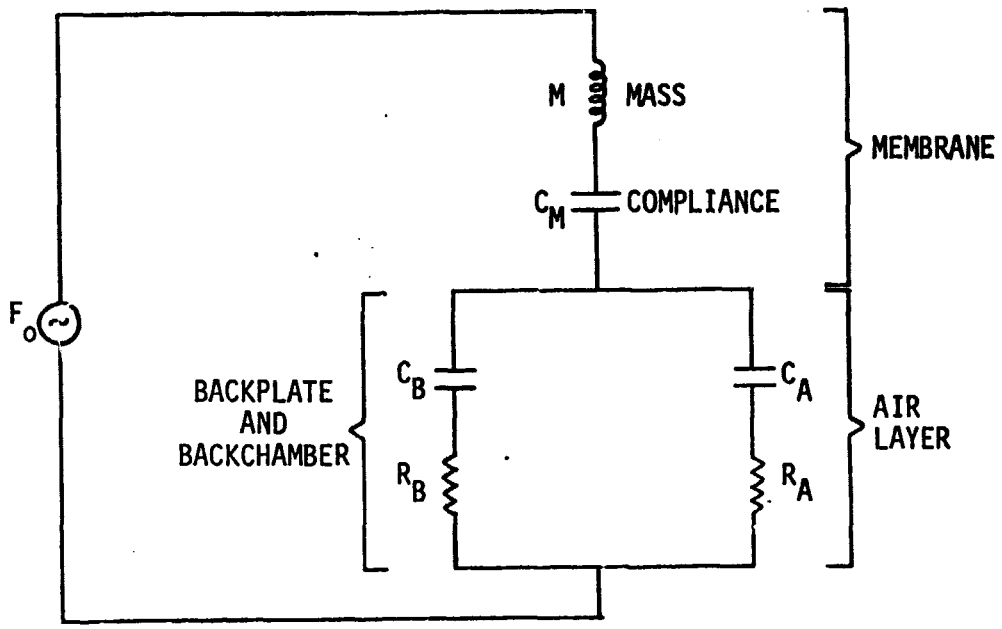

Figure 4. Equivalent circuit of prototype condenser microphone: $M = 826\ kg/m^4$, $C_M = 6.82 \times 10^{-14}\ m^5/N$, $C_A = 4.31 \times 10^{-14}\ m^5/N$, $R_A = 6.7 \times 10^6\ N\ sec/m^5$, $C_B = 1.5 \times 10^{-12}\ m^5/N$, $R_B = 1.3 \times 10^{}\ N\ sec/m^5$.

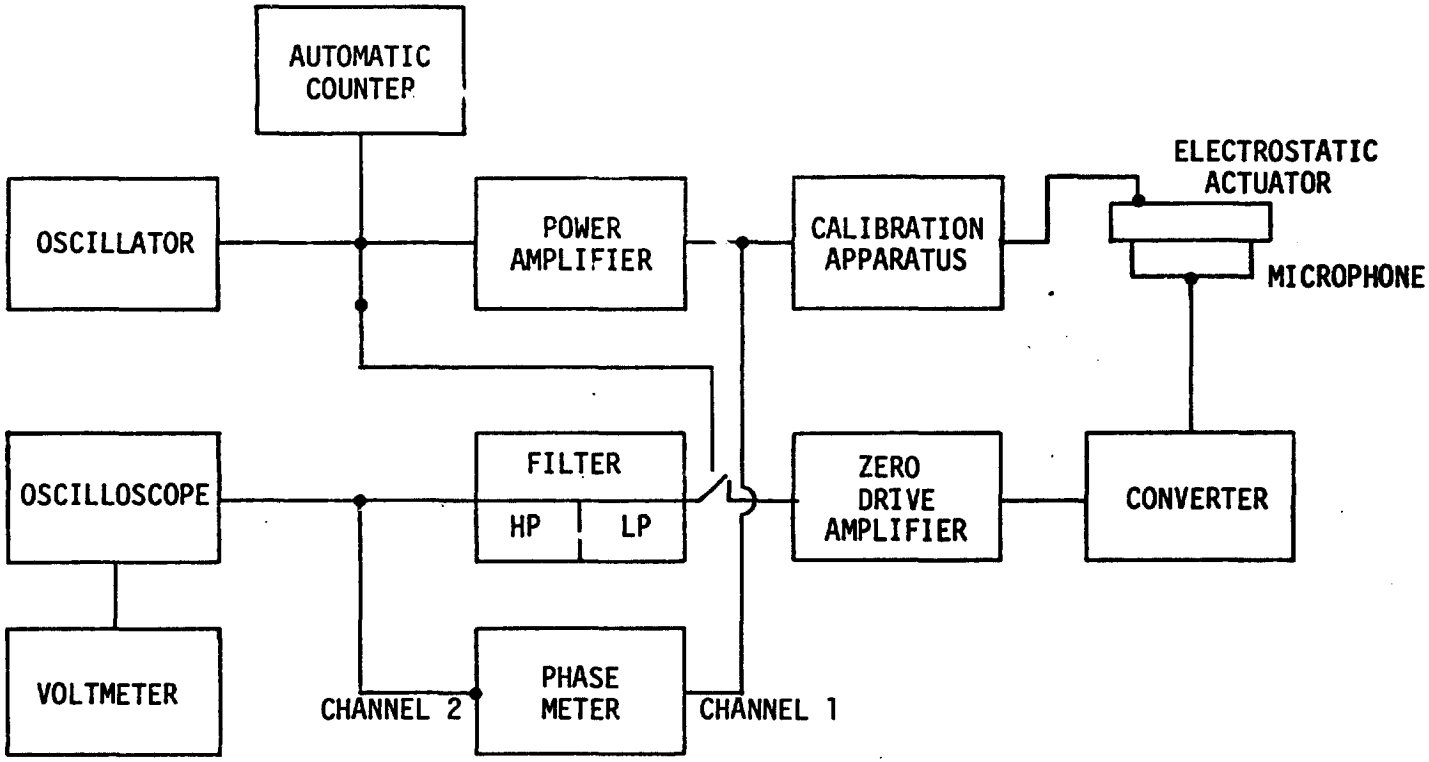

Figure 5. Instrumentation used to measure microphone frequency response: oscillator = HP model 651B; automatic counter = HP model 5323A; power amplifier = HP model 467A; calibration apparatus = B & K type 4142; electrostatic actuator = B & K type UA0033; converter (see reference 7); zero drive amplifier = MB Electronics type N461 with modifications (see reference 7); filter = Kronhite model 3202; oscilloscope = Tektronix type 549 with 1A7A plug-in; voltmeter = HP model 3403C; phase meter = Ad-Yu Electronics type 405L.

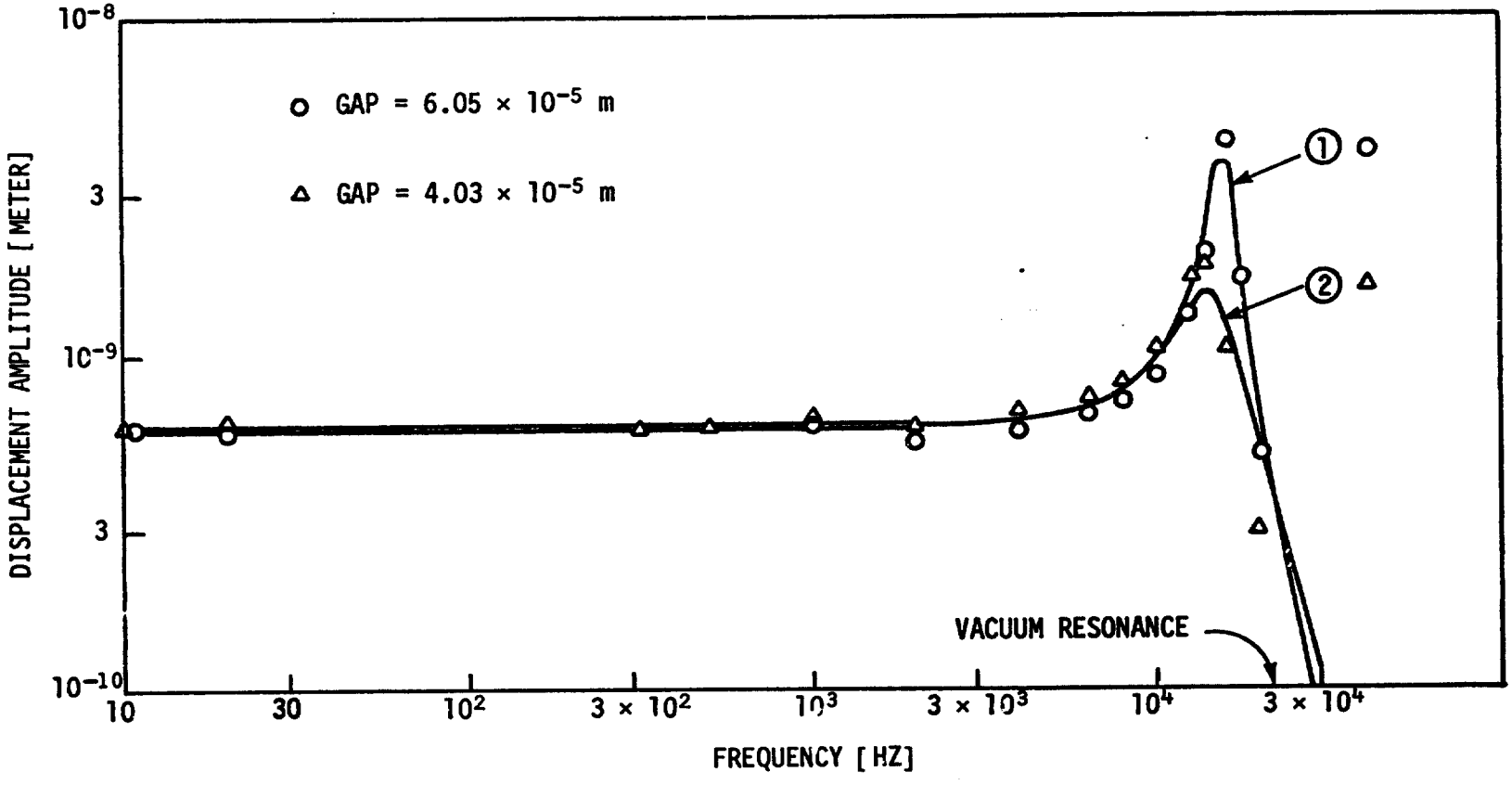

Figure 6. Frequency dependence of membrane displacement amplitude for two different gap distances: theoretical curve (case 2): ———; experimental points: O and Δ. Tension = 2962 N/m.

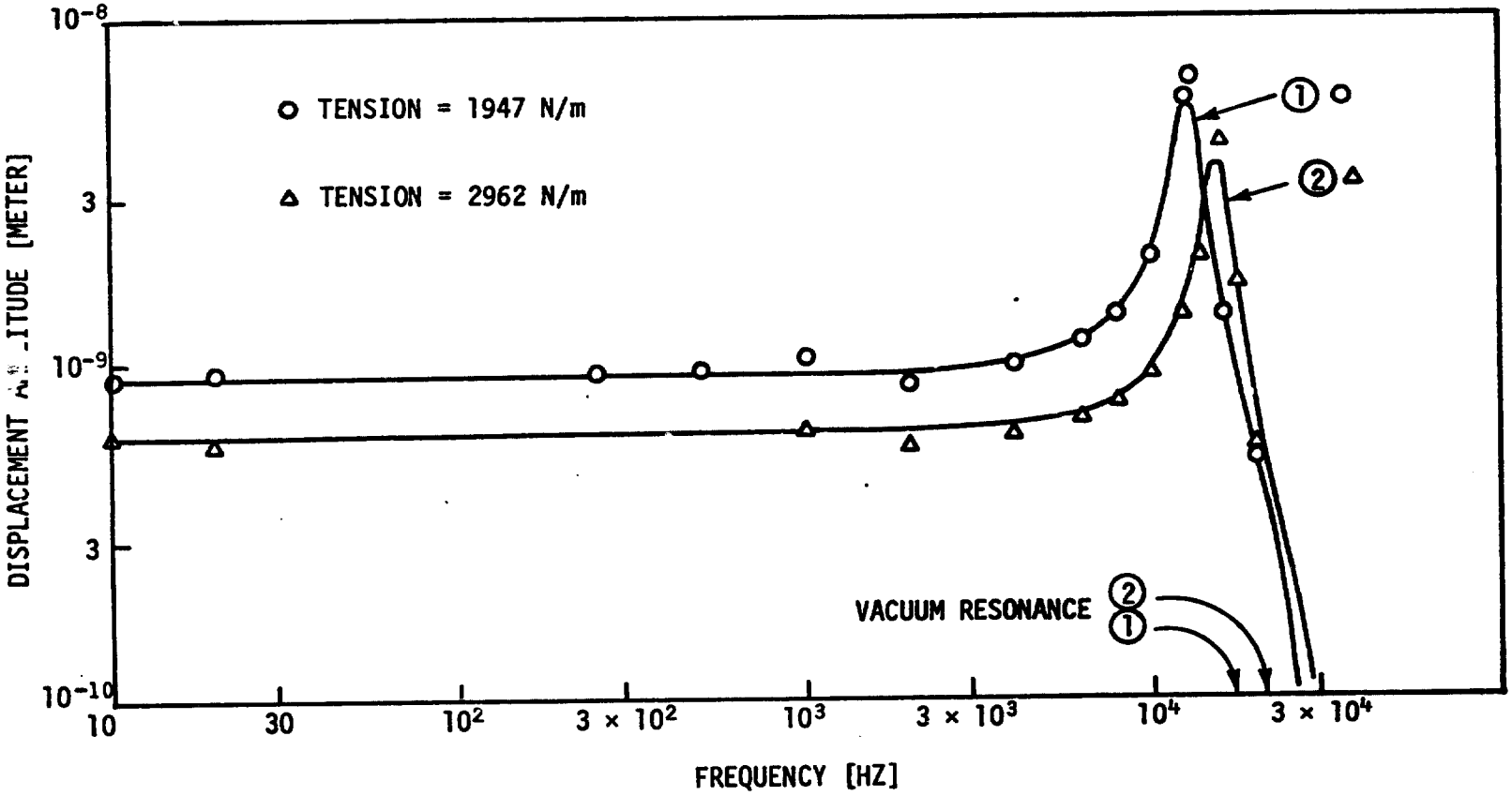

Figure 7. Frequency dependence of membrane displacement amplitude for two different values of membrane tension: theoretical curve (case 2) ·——— ; experimental points: O and Δ . Gap = 6.05×10^{-5} m.

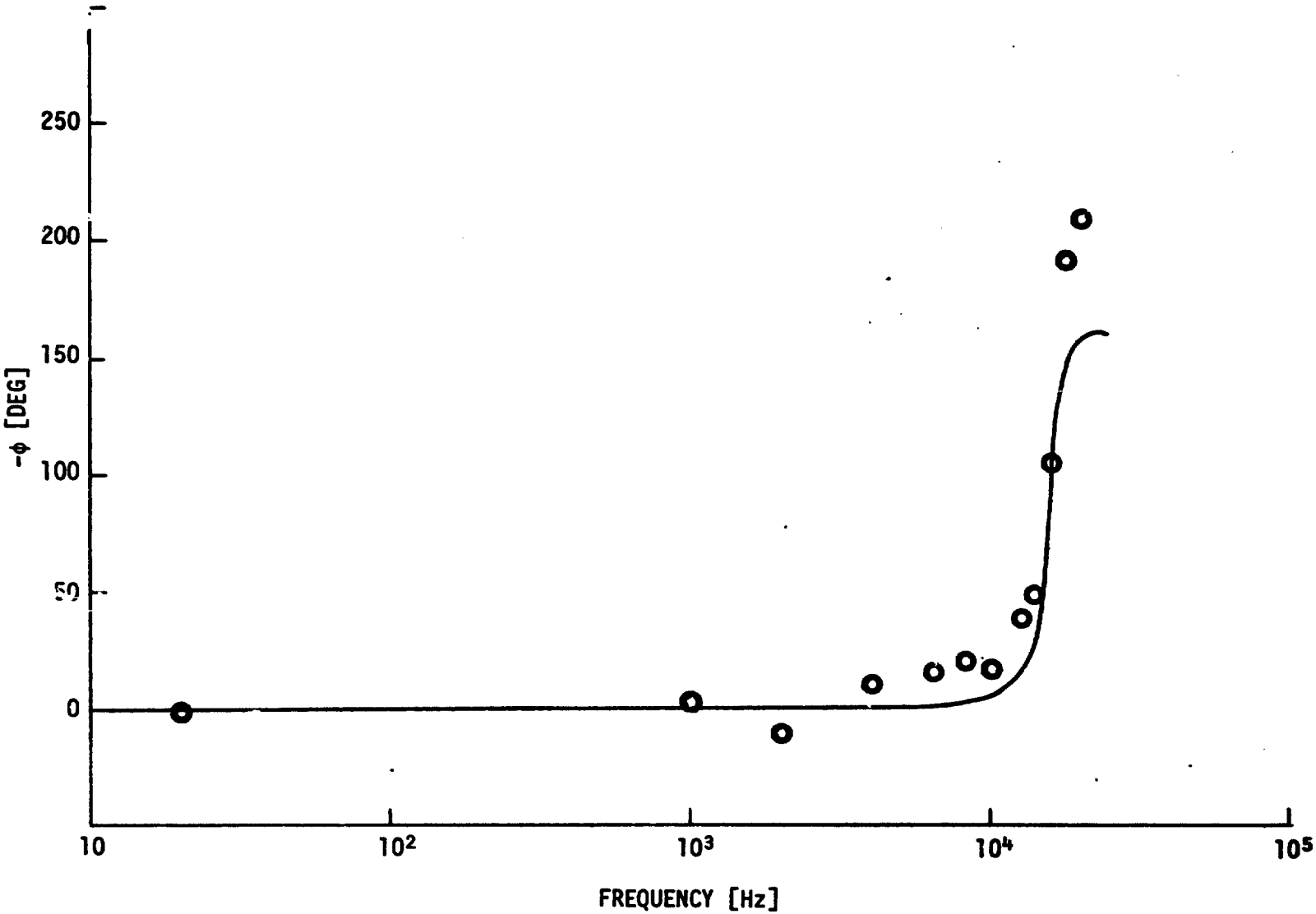

Figure 8. Frequency dependence of phase angle between incident pressure and membrane displacement corresponding to curve ① of figure 6.

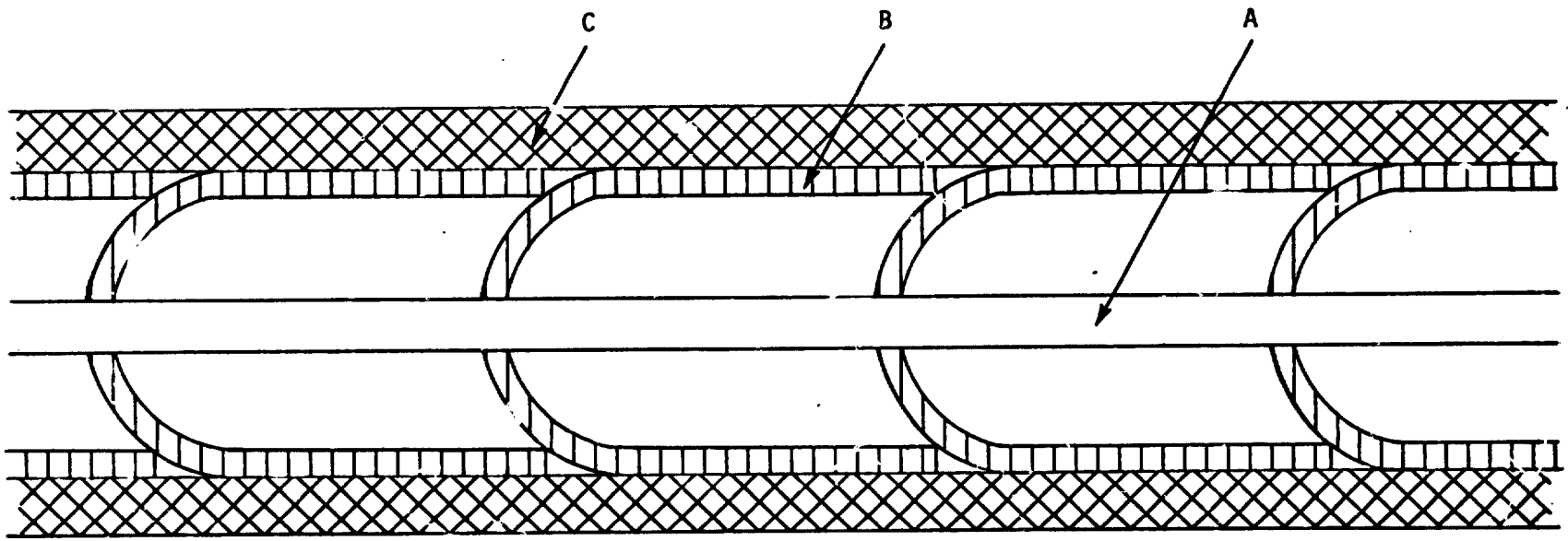

Figure 9. Cross section of high-temperature cable fabricated at Langley Research Center: A = center conductor, B = ceramic beads, C = outer conductor.